# Solid State and Nuclear Results from a Mössbauer-Type Study of $Au^{197}$

LOUIS D. ROBERTS
*Oak Ridge National Laboratory, Oak Ridge, Tennessee*

AND

J. O. THOMSON
*University of Tennessee, Knoxville, Tennessee*

(Received 6 August 1962)

Through the measurement of the hfs of dilute alloys of gold with iron, cobalt, and nickel, the magnetic moment of the first excited state of $Au^{197}$ has been measured as $+0.38\pm0.08$ nm. It was found that the hfs coupling constant in the alloys is closely proportional to the magnetic moment of the host ferromagnetic metal. The value of the effective hyperfine field for the iron alloy is $H'=(1.46\pm0.16)\times10^6$ gauss. A study of the isomer shift of the gold-nickel alloy system as its relates to ferromagnetism is presented. The recoilless absorption linewidth as a function of absorber thickness for metallic gold is given. The half-life of the first excited state of $Au^{197}$ is found to be $T_{1/2}=(1.93\pm0.2)\times10^{-9}$ sec.

## INTRODUCTION

THE measurements to be reported here concern the recoilless radiation from the 77-keV first excited state of $Au^{197}$. The ground state with $I=\frac{3}{2}$ has been assigned in the shell model[1] as $d_{3/2}$ and the excited state with $I^*=\frac{1}{2}$ as $s_{1/2}$. The ground-state magnetic[2] and quadrupole[3] moments have been measured as $\mu=+0.1439$ nm and $q=0.56\times10^{-24}$ cm$^2$, but the excited-state magnetic moment $\mu^*$ has not been measured previously. The 77-keV radiation will then consist of six lines whose positions will reflect the monopole, dipole, and quadrupole interactions between the gold nucleus and its electron environment.

In this work, each of the several aspects of recoilless radiation effects for $Au^{197}$ has been explored in some degree. The quantities relative to which information has been obtained are the 77-keV $\gamma$-ray linewidth at half height $\Gamma$, and thus the half-life $T_{1/2}$ of the 77-keV state; the fraction $f$ of recoilless radiation from the source, or of recoilless absorption $f'$ for the $Au^{197}$ in several solid-state environments; the cross section $\sigma_0$ for the absorption of the recoilless radiation including some information about the conversion coefficient; the so-called isomer shift,[4] i.e., the line position, as a function of atomic environment of the gold; the magnetic polarization of the gold atom in ferromagnetic environments which gives information about the effective magnetic field at the gold nucleus and the magnetic moment of the $Au^{197}$ first excited state. All of the measurements reported here were made at temperatures near 4.2°K.

A number of our results described here in detail have been reported previously in a preliminary way.[5–7] Measurements of some of these quantities have also been reported by Nagle *et al.*[8] and by Shirley and collaborators.[9] Where they overlap, the experimental results obtained by these authors are in general agreement with the measurements reported here. Our results are of somewhat higher resolution and correspondingly our conclusions differ somewhat from theirs in several areas.

## EXPERIMENTAL PROCEDURES

A compact transducer has been developed in which both the $\gamma$-ray source and the absorber may be together held at any desired temperature from the liquid helium region to somewhat above room temperature. In this equipment, Fig. 1, the source is held stationary while the absorber is set in motion. The device has been found to work well in a velocity range in excess of $\pm200$ mm/sec. The oscillating member or armature consists of a brass tube with an alnico bar magnet within. This brass tube–magnet assembly is supported from a relatively heavy and rigidly mounted brass block by two phosphor-bronze leaf springs. This mounting is of such character that the brass tube–magnet assembly moves freely along the direction of the tube axis but other modes of motion are highly suppressed. The absorber is mounted in a carrier at the upper end of the armature and above the source. The source is within a lead housing and the gamma radiation is emitted through a collimator in such a way that all of the radiation of necessity goes through the absorber. The bar magnet is surrounded at each end by a coil and the armature is driven by a small ac current fed to the lower coil. With the apparatus at liquid-helium temperature the driving power was of the order of a few

[1] M. G. Mayer and J. H. D. Jensen, *Elementary Theory of Nuclear Shell Structure* (John Wiley & Sons, Inc., New York, 1955).
[2] H. H. Woodbury and G. W. Ludwig, Phys. Rev. **117**, 1287 (1960).
[3] W. von Siemens, Ann. Physik **13**, 158 (1953).
[4] O. C. Kistner and A. W. Sunyar, Phys. Rev Letters 4, 412 (1960).
[5] L. D. Roberts and J. O. Thomson, Bull. Am. Phys. Soc. **6**, 462 (1961).
[6] L. D. Roberts and J. O. Thomson, Bull. Am. Phys. Soc. **6**, 75 (1961); **6**, 230 (1961); **7**, 351 (1962).
[7] L. D. Roberts and J. O. Thomson, Bull. Am. Phys. Soc. **7**, 350 (1961).
[8] D. Nagle, P. P. Craig, J. G. Dash, and R. R. Reiswig, Phys. Rev. Letters **4**, 237 (1960).
[9] D. A Shirley, M. Kaplan, and P. Axel, Phys. Rev. **123**, 816 (1961).

milliwatts. The velocity was measured by the output voltage from the upper coil. A typical sensitivity was 49.0 mV rms/cm sec. In practice this signal was given a dc bias and amplified. The amplitude $V$ of the amplified ac component was near three volts.

After passing through the absorber the $\gamma$ rays were counted by a NaI-Tl scintillation counter located about 10 in. above the source and at room temperature. The photomultiplier output was amplified by a DD2 amplifier and the pulses corresponding to the 77-keV $\gamma$ were selected by a single-channel analyzer.

The above amplified voltage and the single-channel output pulses were combined in a transistor modulator of a type developed at the Brookhaven National Laboratory.[10] This modulator output then consisted of pulses each of approximately 1-$\mu$sec length and with an amplitude very closely equal to the above amplified voltage at the instant that the given $\gamma$ ray passed through the apparatus. These modulated pulses were then fed to a 200-channel RIDL[11] pulse-height analyzer.

The transducer armature resonant frequency was always within a few cycles of 30 cps depending on the mass of the particular absorber being studied. It was driven at a frequency a few tenths cycle below resonance, and with an amplitude of a few tenths millimeter to a millimeter, depending on the desired velocity range. As measured on a spectrum analyzer the harmonic content of the output voltage $V$ was of the order of a few hundredths percent. The amplitude of the motion was controlled to about 0.5% with a suitable feedback circuit. The noise level on the velocity signal was negligible. Over some months of operation the several aspects of the above system were found to be stable and reproducible and linear to 1% or better.

The number of counts which will appear in a given channel of the RIDL pulse-height analyzer will depend on the time $\Delta t$ that the voltage $V$ spends in passing through an analyzer channel of width $\Delta V$. Then for the sine wave motion of our transducer $V=V_0 \sin\omega t$, and for infinitesimal channel width, we have

$$\Delta t=\frac{V}{[1-(V/V_0)^2]^{1/2}}. \tag{1}$$

At $V\sim 0$ this relation is an excellent approximation even for small but finite channel width, and has been found to hold remarkably well for finite $V/V_0$. Extended studies were made of the behavior of the system without a resonant $\gamma$-ray absorber to see how closely Eq. (1) (and also a more precise relation taking finite channel width into account) would be obeyed. At low counting rates such that the RIDL analyzer dead time was negligible, the system followed the expected behavior within statistical error over the range $0\leq|V|\leq 0.8\ V_0$, but deviated somewhat for $V$ close to $V_0$. With higher counting rates, even within the above velocity range, it was necessary to apply a linear correction to Eq. (1) to take the analyzer dead time into account. In the measurement of a Mössbauer spectrum with an absorber now mounted on the transducer armature, the distribution of counts which would appear in the RIDL pulse-height analyzer would be described, for example, by Eq. (1), but modified by the recoilless absorption. To linearize this distribution of counts, it was sometimes suitable to divide the data by Eq. (1) but it was more often convenient to simply divide the data by the results of a similar run taken without absorber. The Mössbauer absorption minima would then appear as a modulation on a gently sloping straight or possibly slightly curved line. This slope was attributed to a small variation in RIDL analyzer dead-time effects due to small differences between the counting rate in taking the data and the normalization curve. It was removed from the data by one further division by a straight line of suitable slope. These two divisions constitute the treatment given to the experimental points presented here.

In the data presented, positive velocity is defined as motion of the absorber toward the stationary source. Thus, if a resonant absorption line occurs at positive velocity, Doppler energy has been added to the source gamma ray to bring about the resonant condition.

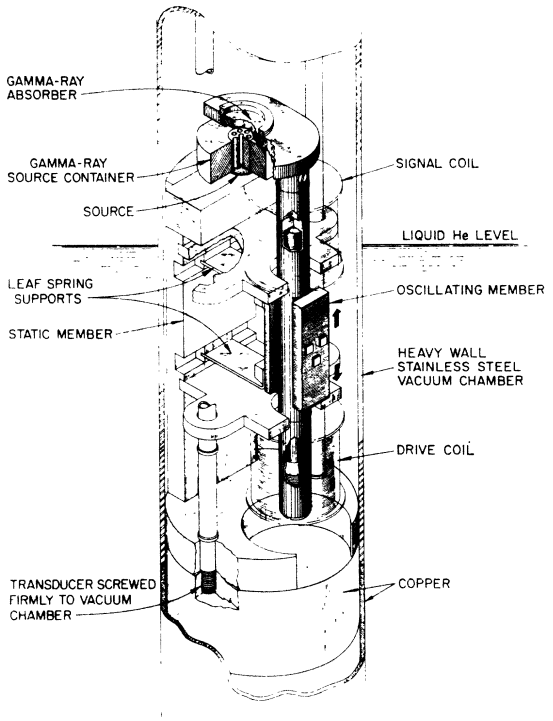


FIG. 1. Sine-wave transducer for Mössbauer experiments down to the helium-temperature region.

[10] O. C. Kistner (private communication).
[11] Radiation Instrument Development Laboratory.

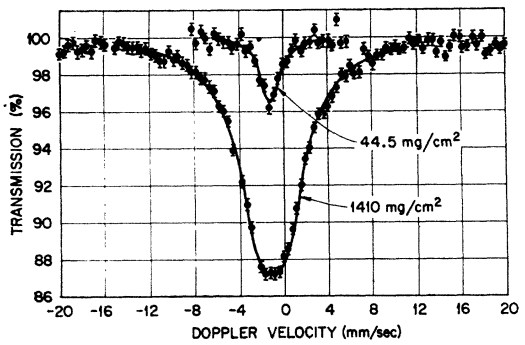


FIG. 2. The percent transmission as a function of Doppler velocity of 77-keV gamma rays from the Pt(Au) source through metallic gold absorbers. The solid curves are theoretical fits to the data points from Eq. (2).

It was generally convenient to accumulate data at a rate of somewhat more than $10^5$ counts per minute input to the multichannel analyzer. This gave roughly $10^5$ counts per channel over 160 channels in 5 h.

The source of the $\gamma$ rays was prepared by activating a 50-mg foil of platinum enriched to 65% in $Pt^{196}$ in the Oak Ridge National Laboratory Research Reactor for 12 h. This source, which we designate Pt(Au) was used in all of the measurements reported here. The gamma radiation from this source contained an appreciable component of gold x ray which was not resolved from the 77-keV $\gamma$ used in these measurements. As will be discussed, an approximate value for the percentage of x ray was obtained using absorption edge techniques.

## PURE GOLD ABSORBERS

A number of experiments were carried out using absorbers made from different thicknesses of metallic gold. The transmission spectra as a function of Doppler velocity for two thicknesses of gold, using a Pt(Au) source are shown in Fig. 2. It may be seen that, for both curves, the isomer shift $\Delta E_0$ for pure gold is $-1.37\pm0.2$ mm/sec$(-2.83\pm0.40\times10^{-3}$ cm$^{-1})$ with respect to the platinum-gold source. Thus, the gamma transition energy for gold in platinum is greater than that for pure gold.

In order to analyze the transmission curves for thick absorbers, it is necessary to evaluate the integral

$$I(T_A,y)=\frac{1}{\pi}\int_{-\infty}^{\infty}dx\,\frac{1}{1+(x-y)^2}\exp\left(-\frac{T_A}{1+x^2}\right). \quad (2)$$

In this equation, $x=2E/\Gamma$ and $y=2\Delta E/\Gamma$, where $\Gamma$ is the Breit-Wigner width, related to the lifetime $\tau$ of the excited state by

$$\Gamma\tau=\hbar, \quad (3)$$

$E$ is the $\gamma$-ray energy, and $\Delta E$ is the energy displacement from resonance. $T_A$ is the effective absorber thickness given by

$$T_A=N\sigma_0 af't, \quad (4)$$

where $N$ is the number of nuclei/mg, $a$ is the isotopic abundance of the isotope used in the experiment, $\sigma_0$ is the cross section for resonant absorption at resonance, $t$ is the source thickness in mg/cm$^2$ and $f'$ is the recoilless fraction in the absorber. A similar source recoilless fraction is designated as $f$.

The Debye theory gives[12]:

$$f \text{ or } f'=\exp\left[-\frac{3}{2}\left(\frac{E^2}{2Mk\theta}\right)\left(1+\frac{4\phi(\theta/T)}{\theta/T}\right)\right], \quad (5)$$

where $\phi(\theta/T)$ is the Debye function[13] and $\theta$ is the Debye temperature. It will be convenient to define

$$t^0=1/N\sigma_0 af' \quad (6)$$

as the $1/e$ absorption thickness.

This integral has been given by Margulies and Ehrman[14] for $T_A$ up to 10. We have extended their calculation up to $T_A=29$ for values of $y$ up to 10. Figure 3 shows some of the results of this calculation. The left-hand scale is the ratio of linewidth at half maximum from Eq. (2) to the natural linewidth. One sees here that the minimum linewidth detectable in this type of measurement is just twice the natural linewidth. The right-hand scale gives the integral $I(T_A,0)$, the transmitted fraction at maximum resonant absorption.

Figure 4 shows the observed linewidth as a function of thickness in mg/cm$^2$ of gold for four metallic gold

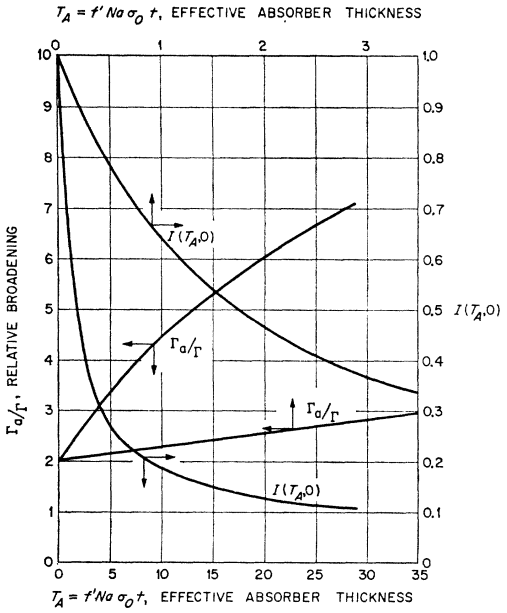


FIG. 3. The linewidth in units of the natural width and $I(T_A,0)$ for thick absorbers.

[12] H. Fraunfelder, *The Mössbauer Effect* (W. A. Benjamin, Inc., New York, 1962).

[13] A. H. Compton and K. Allison, *X-Rays in Theory and Experiment* (D. Van Nostrand Company, New York, 1935), 2nd. ed., p. 437.

[14] S. Margulies and J. R. Ehrman, Nucl. Instr. Methods **12**, 131 (1961).

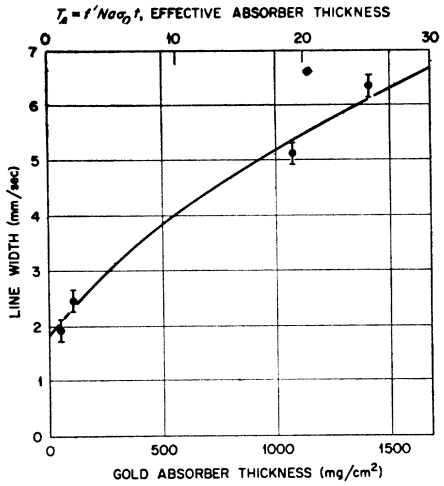


FIG. 4. Absorption linewidth as a function of gold absorber thickness for the four absorbers studied. The solid curve is the best fit to the experimental points from Eq. (2) and Fig. 3. The value of the width at the intercept is twice the natural linewidth.

absorbers. The solid line has been drawn as the best fit to the data using the curve for relative linewidth in Fig. 3. The fitting parameters with their estimated errors are

$$2\Gamma = 1.83 \pm 0.20 \text{ mm/sec},$$

$$t^0 = 56 \pm 4 \text{ mg/cm}^2 \text{ gold}.$$

Here $2\Gamma$ is the linewidth extrapolated to zero absorber thickness.

Using our experimental width $2\Gamma$, one may determine a value for the half-life of the 77-keV state of $T_{\frac{1}{2}} = (1.93 \pm 0.20) \times 10^{-9}$ sec.[5] This is in agreement with the direct half-life measurement of Sunyar of $(1.90 \pm 0.10) \times 10^{-9}$ sec.[15] Implicit in our determination are the assumptions that instrumental broadening was negligible, and that neither quadrupole coupling nor inhomogeneous broadening were present in either source or absorber. It is felt that these assumptions are justified, and that we have observed the natural linewidth.

With the value $t^0 = 56 \pm 4$ mg/cm² and the expression

$$\sigma_0 = 2\pi\lambda^2[(2I^*+1)/(2I+1)][1/(1+\alpha)], \qquad (7)$$

one finds that $f'/(1+\alpha) = (2.83 \pm 0.20) \times 10^{-2}$. In Eq. (7) $\alpha$ is the conversion coefficient for the $\gamma$ transition studied, and $\lambda$ is the reduced $\gamma$-ray wavelength. Using a theoretical estimate of the conversion coefficient $\alpha = 3.96 \pm 0.14$ given by Shirley *et al.*,[9] one finds $f' = 0.14 \pm 0.015$ for the 77-keV gamma ray in gold. This may be compared with $f' = 0.18$ at 4.2°K calculated from Eq. (5) using $\theta_{Au} = 164$°K. From the magnitude of the effect for thick gold absorbers, one may determine the recoilless fraction $f$ in the Pt(Au)source. In order to do this it was necessary to know what fraction of the radiation gating the multichannel analyzer was due to the 77-keV gamma ray. From the results of some absorption edge measurements using a proportional counter, we estimated this fraction to be $0.48 \pm 0.10$. This fraction was, however, modified by the thick absorbers due to the larger absorption of the principal x-ray components at 67 and 69 keV relative to the 77-keV gamma ray. Our estimate for $f$ for the Pt(Au) source, based on the results for thick absorbers is $f_{Pt(Au)} = 0.27 \pm 0.03$ This may be compared to an $f_{Pt(Au)} = 0.30$ at 4.2°K calculated from Eq. (5) by assuming that $\theta_{Au}' = \theta_{Pt} = 233$°K where $\theta_{Au}'$ is an effective Debye constant for gold in the platinum lattice.[16]

[15] A. W Sunyar, Phys. Rev. **98**, 653 (1955).

### Pt Au ABSORBER

One experiment was performed using a 3 at. % gold in platinum absorber. The total alloy thickness was 1168 mg/cm² of which 37.7 mg/cm² was gold. The isomer shift for this alloy with respect to the Pt(Au) source was equal to zero within experimental error. The line showed some extra broadening which may have been due to nearest-neighbor effects. An estimate of $t^0$ for 3 at. % gold in platinum is $28 \pm 5$ mg/cm². Thus, the ratio $f_{AuPt}/f_{Au} = 1.9 \pm 0.4$ independent of background in the 77-keV photopeak. The expected ratio on the basis of the Debye theory, using $\theta_{Pt} = \theta_{Au}' = 233$°K and $\theta_{Au} = 164$°K is 1.65 at 4.2°K.

### MEASUREMENTS WITH $Au^{197}$ IN A FERROMAGNETIC ENVIRONMENT

It was discovered by Samoilov *et al.*[17,18] that when gold and a number of other normally diamagnetic materials are dissolved in iron, the diamagnetic atom may partake of the ferromagnetism of the host. They found, for example, in a nuclear orientation study of $Au^{198}$ dissolved in iron that the gold atom had been magnetically polarized. This polarization was manifested in their work through a hyperfine structure coupling to the $Au^{198}$ nucleus. This coupling may be described as an effective magnetic field $H'$ for which they gave a value in the vicinity of $10^6$ G. This remarkably high $H'$ suggested the possibility of studying solid solutions of $Au^{197}$ in ferromagnetic host materials by the Mössbauer technique. In this section we discuss measurements on a number of ferromagnetic alloy absorbers, alloys of gold with iron, with cobalt, and with nickel.[6]

#### Dilute Alloys of Gold with Iron

Absorbers have been prepared from three different melts containing 1 at. % of gold in iron and from one melt containing ½ at. % of gold in iron. The alloys were melted in an arc furnace which gave a rapid quench

[16] W Marshall (private communication).

[17] B. N. Samoilov, V. V. Sklyarevskii, and E. P. Stepanov, J. Exptl. Theoret. Phys. (U.S.S.R.) **36**, 644 (1959); **36**, 1944 (1959); **38**, 359 (1959).

[18] B. N. Samoilov, V. V. Sklyarevskii, and V. D. Gorobchenko, J. Exptl. Theoret. Phys. (U.S.S.R ) **41**, 1783 (1961).

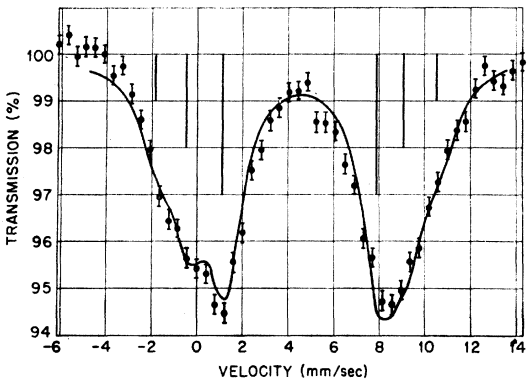


FIG. 5. Gamma-ray absorption as a function of velocity for ½% Au in Fe. The solid line is the fit to the data using Eqs. (8) and (9) with the parameters given in Table I and width 2 Γ.

(less than 1 min) to near room temperature and the samples received no further heat treatment. It was expected that the alloy would be a solid solution. Metallographic studies on several samples showed that these specimens were single phase. All of the measurements made on this group of alloys gave results in excellent agreement; i.e., the spectrum observed gave the same linewidths, line positions and structure within the small statistical errors for the one-half atomic percent and for each of the 1 at. % alloys. Among these samples, the most complete study was made on the ½ at. % sample with 63.9 mg/cm² of Au. The results of this measurement are displayed in Fig. 5.

The $\gamma$-ray absorption as a function of velocity was found to consist of two well separated lines each of these being a triplet. It was found that the triplet at the higher Doppler velocity was slightly narrower than the lower velocity group. As will be discussed below, the doublet spacing is assigned to the excited state of spin ½, the triplet to the ground state of spin ⅜, and the width difference mentioned above is assumed to reflect a small quadrupole interaction.

The locations of the above six lines may then be described in terms of the following Hamiltonians, Eq. (8) for the ground state and Eq. (9) for the excited state, where the effective magnetic field $H'=H_z'$ is assumed to be along the $z$ axis.

$$\mathcal{H}_g=-2\mu H_z'I_z/3+P[I_z^2-I(I+1)/3], \quad (8)$$

$$\mathcal{H}_e=-2\mu^* H_z'I_z^*+\Delta E_I. \quad (9)$$

In Eq. (8), $P$ is the quadrupole coupling constant.

The isomer shift $\Delta E_I$ has been associated somewhat arbitrarily with the excited state. Figure 6 gives a schematic representation of the six transitions between these two states.

The solid line drawn through the experimental points, Fig. 5, is then a sum of six Breit-Wigner functions which are assumed to have the width 2Γ, [Eq. (2) and Fig. 3] and to have intensity ratios 1:2:3:3:2:1. This intensity distribution corresponds to the assumption that the magnetizations of the magnetic domains were random in direction. The sample was sufficiently thin that $\gamma$-ray absorption saturation effects were not expected to affect these intensities or the component linewidths importantly. The locations of these six lines used to fit the experimental points are given in terms of the constants of Eqs. (8) and (9) in Table I.

The above intensity ratio assignment, which describes our measurements quite well, assumes that both $\mu$ and $\mu^*$ have the same sign. This corresponds to a positive magnetic moment, $\mu>0$, for the excited state. As will be seen from Table I, and Figs. 5 and 6, this fit to our data enables one to calculate the ratio of the magnetic moments between the excited and ground states $\mu^*/\mu$. Since $\mu$ is known, we are able to obtain a value for the excited state moment $\mu^*=+0.39\pm0.08$ nm and a value for the effective magnetic field $|H'|=(1.46\pm0.16)\times10^6$ G for Au in Fe.

As mentioned above, the first excited state of $Au^{197}$ has been interpreted as an $s_{1/2}$ state.[1] For such a state our observed moment would be remarkably small, being very far from the Schmidt limit, and suggesting that a pure $s_{1/2}$ configuration cannot be a complete description. The possibility of describing some excited states of odd-$A$ nuclei in terms of excitations of the even-even core has been investigated by de-Shalit.[19]

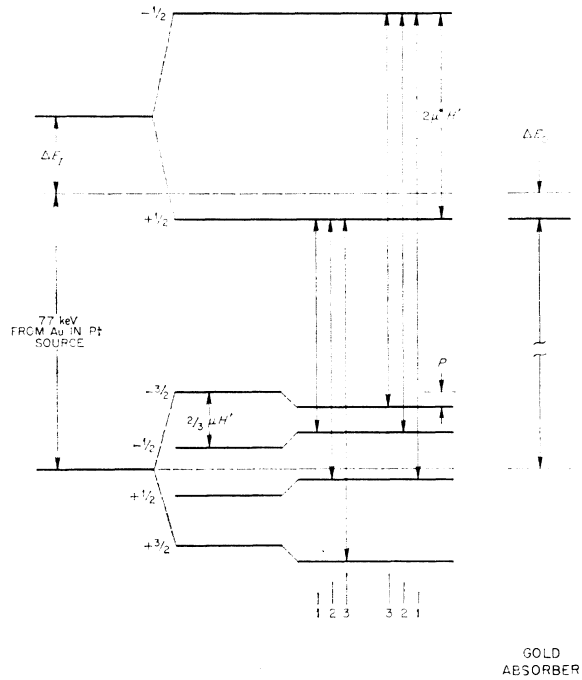


FIG. 6. Nuclear energy levels for the ground and first excited states in $Au^{197}$. The left-hand levels are for a ferromagnetic gold absorber, showing the isomer shift $\Delta E_I$ and the magnetic field and quadrupole splittings. The right-hand level diagram illustrates $\Delta E_0$, the isomer shift between the Pt(Au) source and the pure gold absorber.

[19] A. de-Shalit, Phys. Rev. **122**, 1530 (1961).

TABLE I. Summary of experimental results on ferromagnetic gold alloys. Energies are given in units of $10^{-3}$ $cm^{-1}$.

| | Excited-state splitting $\lvert(\mu^*/I^*)H'\rvert$ | Ground-state splitting $\lvert(\mu/I)H'\rvert$ | $P$ | Isomer shift $\Delta E_I$ | $\lvert H'\rvert$ G[a] | $\mu^*$(nm) |
|---|---|---|---|---|---|---|
| Fe-Au($\frac{1}{2}$%) | 29.1±0.6 | 3.55±0.40 | −0.13±0.08 | 9.5±0.3 | (1.46±0.16)×$10^6$ | +0.39±0.08 |
| Co-Au(1%) | 22.7±0.6 | 2.87±0.30 | −0.21±0.08 | 9.2±0.3 | (1.18±0.12)×$10^6$ | +0.38±0.08 |
| Ni-Au(1%) | 8.2±0.6 | 1.30±0.40 | ··· | 8.4±0.3 | (0.53±0.16)×$10^6$<br>(0.42±0.12)×$10^6$[b] | +0.30±0.15 |

[a] Calculated from ground-state splitting and $\mu=0.1439$ nm.
[b] Calculated from excited-state splitting and $\mu^*=0.39$ nm.

Several values have been given previously for this effective field. In their most recent work on the orientation of $Au^{198}$ nuclei in a dilute gold-iron alloy, Samoilov *et al.*[17] have given a value of $-1.0\times10^6$ G. Using a similar method Kogan *et al.*[20] have given a value $|H'|\geq2\times10^6$ G. Because of more precise thermometry, the best value for $H'$ based on the nuclear orientation of $Au^{198}$ would seem to be the recent result of Stone and Turrell.[21] They give $1.4\times10^6\leq|H'|\leq1.8\times10^6$ G. Their result and our measurement are in quite reasonable agreement.

As was noted above, the two triplet components, Fig. 5, are of different width. This could conceivably arise from a combination of a small spread in $H'$ over the gold atoms in the sample with a correlated distribution in isomer shift $\Delta E_I$. A more natural assumption is that the width difference is due to quadrupole coupling and correspondingly, a term of this form has been introduced into the ground-state Hamiltonian Eq. (8). This is permissible in that the ground-state nuclear spin is $\frac{3}{2}$ (i.e., greater than $\frac{1}{2}$).

One would not at first expect a quadrupole splitting in the dilute iron alloy since pure iron is cubic. The gold atomic size is larger than that of iron, however, and thus the dissolved gold will strain the iron crystal lattice, leading in some degree to a quadrupole coupling effect on other gold atoms near by. Furthermore, small line broadening effects, which are ascribed to a quadrupole interaction, are found in nuclear resonance studies of cubic copper alloys containing small amounts of a number of other metals.[22] This has been discussed theoretically[23,24] in terms of a disturbance or modulation of the Fermi surface of the host metal by an impurity, leading to a quadrupole coupling effect even at somewhat distant neighbors. The magnitude of the quadrupole splitting which we have assumed in order to describe our results is similar to that found for these copper alloys.

The form of Eq. (8) assumes the quadrupole and magnetic tensors to be co-axial. This is surely not the case, but rather the quadrupole tensor axis must assume a distribution of directions relative to the magnetic field. This corresponds to the fact that a line joining nearest Au impurity sites in the Fe lattice will be distributed in direction relative to the direction of magnetization of the iron ferromagnetic domain. Thus, the form of the quadrupole interaction introduced in Eq. (8) is probably only approximate. There will be a distribution of $P$ values and the value given, Table I, will be an average. In drawing the solid curve, Fig. 5, (and also in Figs. 7 and 8 to follow), a sharp value for $P$ was assumed. The fact that this theoretical curve gives a somewhat more sharply defined structure than is observed may then be due at least in part to the fact that a distribution in $P$ was not used.

## Dilute Gold-Cobalt Alloys

Two alloy samples, each consisting of 1 at. % of gold in cobalt have been studied. As with the gold-iron system, the melts were made in an arc furnace, and were rapidly quenched (about 1 min) from the melting point to near room temperature. There was no further heat treatment of the samples. It was expected that the sample would be a solid solution. A section from one of these melts was examined metallographically and was found to be single phase.

All of our recoilless radiation studies on these samples were in good agreement. Figure 7 gives results on one of the gold-cobalt absorbers which contained 112 mg/$cm^2$ of gold. The qualitative character of this result is very similar to that for gold in iron. From the closer doublet spacing, $H'$ is evidently smaller but the quadrupole coupling effect is seen to be somewhat larger. Each of the latter facts seems reasonable in that the magnetic moment of the host cobalt metal is less than that of iron while the predominantly hexagonal structure of cobalt could perhaps result in a larger quadrupole coupling effect than in the case of the essentially cubic iron alloy. Also the gold concentration is a factor of 2 larger in the cobalt than in the iron alloy which would lead to an enhanced effect of gold neighbors. The solid curve gives a fit to the data points again using the width $2\Gamma$, Eq. (2), Fig. 3, and the 1:2:3:3:2:1 intensity ratios. This fit was made quite independently of the fit made to the iron-gold data. The results are summarized in Table I. It will be seen that the mag-

[20] A. V. Kogan, V. D. Kul'kov, L. P. Nikitin, N. M. Reinov, I. A. Sokolov, and M. F. Stel'makh, J. Exptl. Theoret. Phys. (U.S.S.R.) **40**, 109 (1961).
[21] N. J. Stone and B. G. Turrell, Phys. Letters **1**, 39 (1962).
[22] T. J. Rowland, Phys. Rev. **119**, 900 (1960).
[23] W. Kohn and S. H. Vosco, Phys. Rev. **119**, 912 (1960).
[24] C. P. Flynn and E. F. W. Seymour, Proc. Phys. Soc. (London) **76**, 526 (1960).

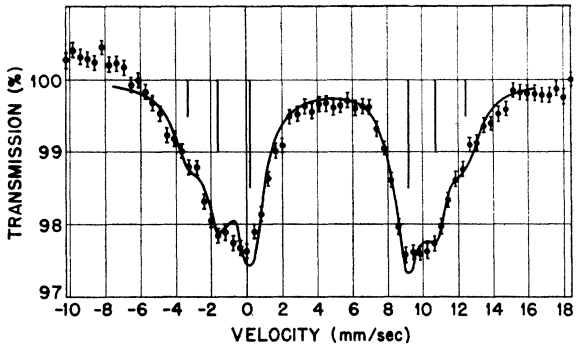


FIG. 7. Gamma-ray absorption as a function of velocity for 1% Au in Co. The solid line is the fit to the data using Eqs. (8) and (9) with the parameters given in Table I and width 2 Γ.

netic moment $\mu^*=+0.38\pm0.08$ obtained here is in good agreement with our $\mu^*$ value from the iron-gold alloy.

### Dilute Alloys of Gold with Nickel

Two dilute alloy samples, each consisting of 1 at. % of gold in nickel have been investigated. As with the iron and cobalt alloys the melts were made in an arc furnace, were rapidly quenched to near room temperature, and received no further heat treatment. A metallographic examination showed that a section from one of the samples was single phase.

The $\gamma$-ray transmissions as a function of velocity measured on these samples were in good agreement. Fig. 8 shows results on a gold-nickel absorber with 70.3 mg/cm$^2$ of gold. Once more the solid curve represents a fit to the data assuming the 1:2:3:3:2:1 intensity ratios and taking the width 2Γ for each of the six component lines. In this case $H'$ and thus the over-all splitting was much smaller than for the iron and cobalt alloys described above. Because of this the quadrupole coupling (although probably present) was not observable and was thus omitted from Eq. (8) in fitting the data points, Fig. 8 and Table I. Because the splitting of the triplet components of the absorption spectrum is here relatively small compared to the width of a component line, the value which we obtain for $H'$ and $\mu^*$ from the gold-nickel alloys is less precise than for the iron and cobalt systems. On the other hand, $|\mu^*H'/I|$ is still relatively well determined. The value for $H'$ found here is the smallest of the values for the three alloys, reflecting the fact that metallic nickel has the smallest magnetic moment of the three host metals.

### Summary of Measurements for Dilute Ferromagnetic Gold Alloys

We would first like to call attention (Table I) to the quite large values found for the isomer shift $\Delta E_I$ for the iron, cobalt, and nickel alloys. In that the same $\gamma$-ray source was used for all of the measurements, this isomer shift is proportional within an additive constant to the $s$-state density $\sum_{n=1}^{6}\psi_{ns}^2(0)$ at the Au$^{197}$ nucleus in the alloys. The behavior of $\sum_{n=1}^{6}\psi_{ns}(r)$ will be reflected in $\sum_{n=1}^{6}\psi_{ns}^2(0)$ and thus in the isomer shift. The values for $\Delta E_I$ given in Table I are relative to the metallic platinum source. It would be more appropriate to consider the shifts $\Delta E_I'$ relative to metallic gold. These shifts may be obtained by adding the isomer shift $\Delta E_0$ obtained for the platinum source and a metallic gold absorber to the values $\Delta E_I$ given for the alloys in Table I. For the dilute iron, cobalt, and nickel alloys these $\Delta E_I'$ values are $12.3\pm0.3$, $12.0\pm0.3$, and $11.2\pm0.3$, in units of $10^{-3}$ cm$^{-1}$. Although these values do differ by amounts somewhat outside their experimental error and seem to show a slight trend with increasing $Z$, emphasis should perhaps be placed on their relative constancy. This seems noteworthy in view, for example, of the facts that iron, cobalt, and nickel have different crystal structures, and are quite different with respect to their 3$d$ band structure.

In Fig. 9 we give a plot of the splitting of the excited state $|\mu^*H'/I|$ for the dilute iron, cobalt, and nickel alloys vs the electronic magnetic moment of the host metals, i.e., 2.22, 1.72, and 0.606 $\mu_B$, respectively. The absolute value of this splitting and thus of the effective field $H'$ is seen to fall on a straight line. This linear behavior implies that a kind of magnetic polarizability of the gold is in some sense a constant.

In a qualitative way, one would expect that $\sum_{n=1}^{6}\psi_{ns}^2(0)$ on the gold would be sensitive to both the 5$d$ and 6$s$ amplitude, presumably increasing if the 5$d$ amplitude is decreased and decreasing with a decrease of 6$s$ amplitude.[25] Gold has ten $s$ electrons in closed shells with only one 6$s$ electron in the conduction band. In the dilute ferromagnetic alloys of gold, above, a major contribution to $H'$ probably arises from the polarization of the spin density of these inner shells. However, a preliminary study suggests that the inner

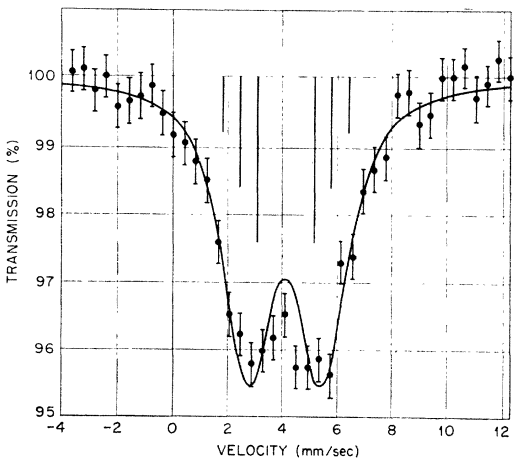


FIG. 8. Gamma-ray absorption as a function of velocity for 1% Au in Ni. The solid line is the fit to the data using Eqs. (8) and (9) with the parameters given in Table I and width 2 Γ.

[25] L. R. Walker, G. K. Wertheim, and V. Jaccarino, Phys. Rev. Letters 6, 98 (1961).

closed $s$ shells do not give a major contribution to the isomer shift.

Returning now to Fig. 9, it is interesting to observe that since $\sum_{n=1}^{6}\psi_{ns}^2(0)$ is nearly constant for the above ferromagnetic gold alloys, it must be the polarization of this essentially constant $s$-state density which varies very nearly linearly with the host magnetic moment for the three alloys. Presumably this polarization must be communicated to the gold atom predominantly by way of its $6s$ shell, but whether this $6s$ shell is polarized through interaction with the host $4s$ electrons, $3d$ electrons, or some hybridization of these is less clear.

As measured by the atomic beam method, the hfs coupling constant for atomic gold ($6s\ ^2S_{1/2}$) is 6099.309 Mc/sec.[26] From this and from the nuclear moment $\mu=+0.1439$,[2] one may calculate for the free gold atom in a strong external magnetic field an effective field of $H_a'=20.9\times10^6$ G. Thus, for gold dissolved in iron, the effective field at the gold nucleus is 7.0% of that arising in the free atom through core polarization and directly from the unpaired $6s$ electron. If the core polarization effects in the free gold atom and those in the alloy should each be proportional to the unpaired $6s$ spin density, $H'/H_a'$ would give a direct measure of this unpaired spin density in the $6s$ shell of the gold atom in the alloy.

## THE $s$-STATE DENSITY IN CONCENTRATED GOLD-NICKEL ALLOYS

Alloys of gold with nickel fall within a class of alloys of which the copper-nickel system may be regarded as the prototype. In a general way one might expect considerations presumably applicable to the copper-nickel system to carry over to gold-nickel.

The copper-nickel alloy system has often been investigated experimentally and theoretically. This solid-solution system has the interesting property that the ferromagnetic moment and Curie temperature decrease linearly with increasing copper content, becoming zero

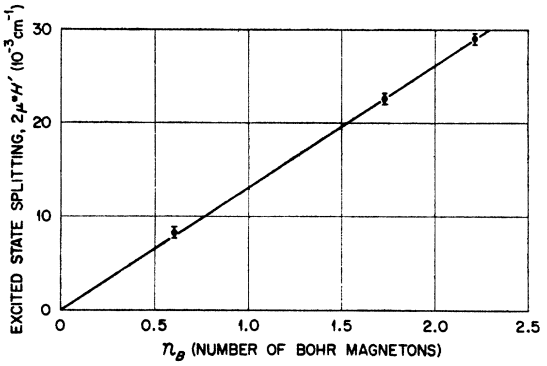


FIG. 9 The magnetic splitting $|2\mu^*H'|$ in units of $10^{-3}$ cm$^{-1}$ as a function of atomic magnetic moment of the ferromagnetic host metal in Bohr magnetons.

[26] G. Fricke, S. Penselinn, and E. Recknagel, Naturwissenschaften 47, 129 (1960).

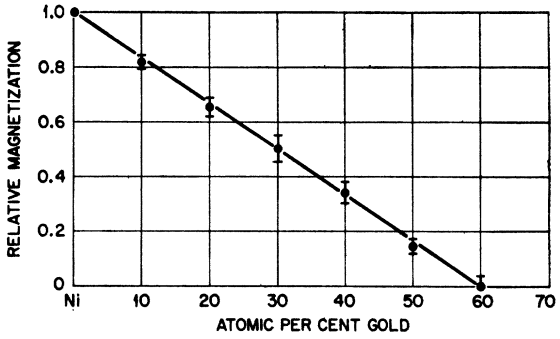


FIG. 10. The relative magnetization in a field of 1.1 kg of gold-nickel alloy samples at 4.2°K as a function of composition. The magnetization of alloys containing 60 at. % or more of gold was zero within our experimental error.

at about 60 at. %. This behavior has been described theoretically as due to a partial transfer of electron charge from the copper $s$ state to the nickel $d$ state, gradually filling the latter as the copper percentage is increased, and thus attenuating the ferromagnetic properties of the substance. In a theoretical discussion of this alloying process using the rigid-band model, Wohlfarth[27] gave a prediction of the behavior of the $s$-state density on the copper atoms. In the understanding of the magnetic behavior of these alloys, the $s$-state density on the copper is clearly of comparable importance to the $d$-band filling. Until the advent of the Mössbauer method, however, no experimental technique was available to measure the $s$-state wave function density. The Mössbauer method gives information about this for suitable nuclei, the isomer shift being proportional within an additive constant to the $s$-state density at the Mössbauer nucleus, see Eq. (10), below.

Unfortunately, there is no copper nucleus suitable for Mössbauer effect studies. However, as we have seen, the 77-keV gamma ray of $Au^{197}$ gives a conveniently measurable Mössbauer effect, and the gold-nickel alloy system has magnetic properties which are very similar to those of copper-nickel. We have made a study of the gold-nickel system for a series of 11 gold-nickel alloy compositions.

In iron and cobalt alloys with gold, the solubility of gold has a maximum value near 1 at. % gold. The gold-nickel system, however, forms solid solutions over the entire composition range at temperatures near 900°C.[28] If these alloys are quenched to room temperature they retain their single phase character. Previous studies have shown that the magnetic properties of these quenched alloys are similar to those of the copper-nickel system.[29]

The alloys which we have studied were melted in an arc furnace. Absorber foils of suitable diameter and thickness were cut from the alloys. These were held in

[27] E. P. Wohlfarth, Proc. Roy. Soc. **A195**, 434 (1948).
[28] M. Hansen, *Constitution of Binary Alloys* (McGraw-Hill Book Company, Inc., New York, 1958).
[29] V. Marian, Ann. Phys. 7, 459 (1937).

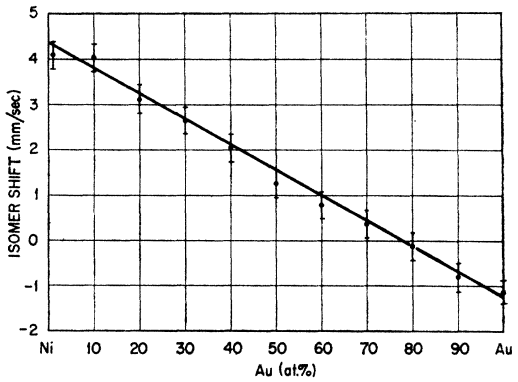


FIG. 11. The observed isomer shift as a function of composition for gold-nickel alloys. The solid line has been drawn to show the linearity of the data.

vacuum at 900°C for one week and then water quenched. After this the samples received no further thermal or mechanical treatment. Table II lists the absorber compositions and thicknesses.

Figure 10 shows the relative magnetization per atom of nickel measured at 4.2°K in a field of 1100 G for our set of Au-Ni alloys. The magnetization is plotted as a function of composition. It is seen that the ferromagnetic moment falls linearly with increasing gold content becoming zero within experimental error at 60 at. % gold and remaining essentially zero on this scale for greater gold percentages.

When gold is alloyed with nickel, the Mössbauer line for gold may be expected to shift and to broaden. The shift corresponds to the change of the $s$-state density at the gold nucleus. The broadening arises from magnetic effects (Zeeman splitting, for example) and from a variation of $s$-state density from atom to atom. In the most simple rigid-band picture, there would be no broadening of the latter type.

In these measurements the same Pt(Au) source as above was used and the temperature of both source and absorber was as usual 4.2°K.

Figure 11 shows the isomer shift as a function of composition for the eleven alloys studied. Although there is some evidence for a slight curvature, the data points are seen to fall along a straight line within statistics. For solutions, including solid solutions, it is found that many physical properties will be a linear or near linear function of composition. For example, the lattice parameter varies nearly linearly by about fifteen percent from pure nickel to pure gold in the present alloy system. The interest in our result then lies in the comparison of the $s$-state density with the magnetic properties. There is very little evidence indeed for any change of trend of the isomer shift (and thus of the $s$-state density at the gold nucleus) with composition in the vicinity of 60% gold where the trend of the magnetic behavior changes abruptly. This departs from a simple interpretation of the rigid band picture that near 60% gold there should be an appreciable change of slope in

TABLE II. Nickel-gold alloys.

| At. % Au | mg/cm² Au |
|---|---|
| 1 | 70.3 |
| 10 | 97.3 |
| 20 | 102.9 |
| 30 | 100.8 |
| 40 | 68.6 |
| 50 | 93.8 |
| 60 | 104.3 |
| 70 | 114.1 |
| 80 | 118.3 |
| 90 | 120.6 |
| 100 | 105.0 |

the dependence of the $s$-state density on composition.[27] This near linear behavior of the isomer shift does not necessarily invalidate the usual concept that in some degree charge is transferred from the gold to the nickel in the alloy. Our result, however, further indicates a required modification of the rigid-band picture. Blandin, Daniel, and Friedel[30] have demonstrated the importance of screening effects in the discussion of the Knight shift in dilute alloys. It may be that similar effects are of importance in the description of our results which depend on an integral of the $s$-state density over the band structure.

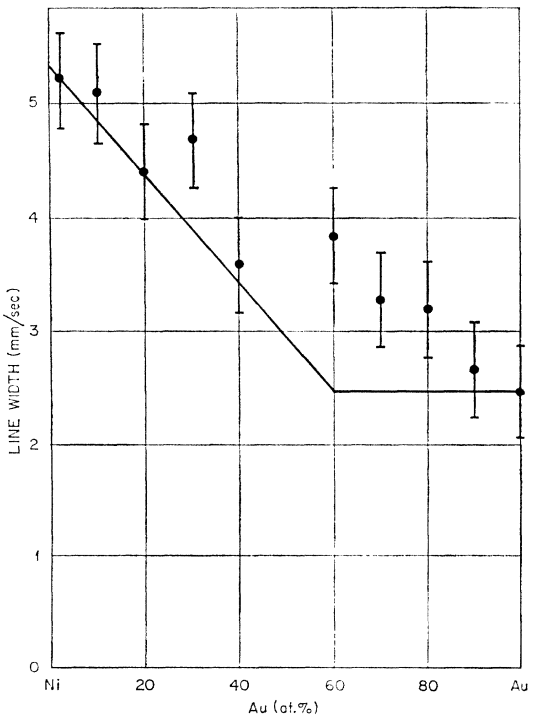


FIG. 12. The observed linewidth as a function of composition for gold-nickel alloys. The solid curve is explained in the text. The widths are the observed values and have not been corrected to a standard absorber thickness.

[30] A. Blandin, E. Daniel, and J. Friedel, Phil. Mag. **4**, 180 (1959); A. Blandin and E. Daniel, J. Phys. Chem. Solids **10**, 126 (1959).

Figure 12 gives a quite preliminary result for the observed absorption linewidth as a function of composition. These widths have not been corrected for gold absorber thickness, Table II. In the interpretation of these widths a knowledge of the recoilless fraction $f'$ in the absorber as a function of composition is required. These measurements of $f'$ have not been made for gold in nickel. At the nickel-rich end, the width given is the over-all width at half-height of the transmission minimum Fig. 8 for the 1 at. % gold alloy. Here we feel that the width is predominantly due to Zeeman splitting along with the natural width, with but relatively little contribution from thick absorber effects. For pure gold, on the other hand, the observed width is the natural width as broadened by absorber thickness. The solid line in Fig. 12 gives a very crude interpolation of some interest. The width associated with the relatively thick pure gold absorber is extended at an assumed constant value to 60% Au. The sloping line extending from this point to the nickel-rich end approximately represents the effect of a linearly rising effective field $H'$ associated with the linearly rising magnetization of the alloy, Fig. 10. This crude model accounts for most of the width.

The difference between this curve and the data points suggests a degree of inhomogeneous broadening. Interestingly, this difference can be roughly represented by $kx(1-x)$, where $x$ is the composition and $k$ is a constant. The rigid band picture would not predict an inhomogeneous broadening of this kind.

## THE ISOMER SHIFT

One of the most interesting aspects of recoilless radiation studies is the isomer shift. As we have mentioned above, this shift reflects the $s$-state density at the nucleus. In a more detailed way, first-order perturbation theory gives the result

$$\Delta E_I \propto (\langle r_g^{2\rho}\rangle - \langle r_e^{2\rho}\rangle)\{[\psi^2(0)]_{\text{source}} - [\psi^2(0)]_{\text{absorber}}\}, \quad (10)$$

where $\langle r_g^{2\rho}\rangle$ is an average over the ground-state nuclear charge distribution. In a single-particle model of an odd-proton nucleus, such as $Au^{197}$,

$$\langle r_g^{2\rho}\rangle = \int_0^\infty \varphi_g^* \varphi_g r^{2\rho} d\tau, \quad (11)$$

where $\varphi_g$ is the single-particle ground-state nuclear wave function. There is a similar integral $\langle r_e^{2\rho}\rangle$ for the excited state of the nucleus. Here one has $\rho = (1-\alpha^2 Z^2)^{\frac{1}{2}}$ with $\alpha$ the fine structure constant and $Z$ the nuclear charge. In the above we have emphasized the value of this shift in giving information about the $s$-state density $\psi^2(0)$. Information about ground- and excited-state nuclear configurations is also reflected in this shift through $\langle r^{2\rho}\rangle$.

Shirley[31] has given an interesting discussion of this shift for $Au^{197}$ based on experimental results[9] similar to ours for dilute alloys of gold in platinum, iron, cobalt, and nickel. He has used in his discussion single-particle ground-state and excited-state wave functions for both square well and Woods-Saxon potentials, and a suggestion of Zeldes[32] that these states are hole states. From these considerations, and the 6$s$ state density at the nucleus for the free gold atom (determined from hfs measurements), he finds the result that relative to metallic gold, the gold atom gains of the order of one 6$s$ electron when placed in iron, cobalt, or nickel. The sign of his result depends, of course, upon whether the 77-keV transition involves a hole or a particle.

A gain of $s$-state charge by gold when alloyed with iron, cobalt, and nickel is somewhat unexpected in terms of the usual solid-state picture of the magnetic properties of these alloys. Several mechanisms which could contribute to an increase of the $s$-state density at the gold nucleus in these alloys are the suggested decrease of the Au–Au distance in the alloy relative to metallic gold[33] and the possibility of a sensitive effect on the isomer shift of the gold $d$-state wave function through screening[25] of the $s$ electrons.

One may not be compelled to accept this increase of $s$-state density, however. The nuclear configuration for $Au^{197}$ suggested by Zeldes[32] and assumed by Shirley in his calculation[31] would correspond to a much larger magnetic moment for the excited state than we observe. Our smaller observed moment evidently will lead to a different nuclear configuration. As was mentioned above, the possibility that the excited-state configuration for $Au^{197}$ may involve an excitation of the even-even core has been suggested by de-Shalit.[19]

For a sequence of core levels of rotational character one would expect, in first approximation, that the core moment of inertia and thus the core dimensions would be constant. To the degree that this is so, there would be no isomer shift. Thus, both the large isomer shift and the small excited-state magnetic moment will effectively serve to limit the possible choice of configurations.

## ACKNOWLEDGMENTS

We are happy to acknowledge numerous discussions of this work with G. R. Satchler and with E. O. Wollan. We appreciate the help of A. R. Brosi, M. L. Pickelsimer, and H. S. Pomerance in some of the measurements.

[31] D. A. Shirley, Phys. Rev. **124**, 354 (1961).
[32] N. Zeldes, Nucl. Phys. **2**, 1 (1956/57).
[33] P. A. Flinn, B. L. Averbach, and M. Cohen, Acta Met. **1**, 664 (1953).

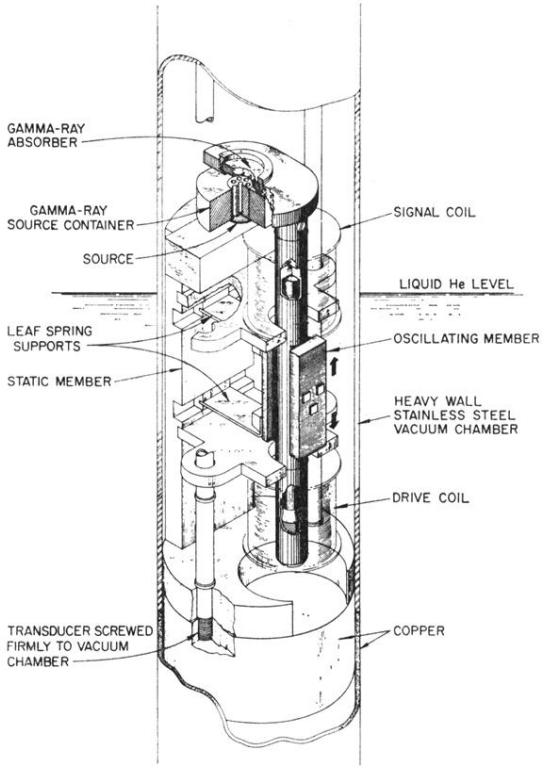


FIG. 1. Sine-wave transducer for Mössbauer experiments down to the helium-temperature region.